ACADEMIC PRESS

Available online at www.sciencedirect.com

SCIENCE DIRECT®

Journal of Solid State Chemistry 175 (2003) 72–83

JOURNAL OF SOLID STATE CHEMISTRY

http://elsevier.com/locate/jssc

Selectivity for Cs and Sr in Nb-substituted titanosilicate with sitinakite topology

Akhilesh Tripathi,[a] Dmitri G. Medvedev,[b] May Nyman,[c] and Abraham Clearfield[a,*]

[a] *Department of Chemistry, Texas A & M University, College Station, TX 77842-3012, USA*
[b] *Department of Nuclear Engineering, Texas A & M University, College Station, TX 77843-3133, USA*
[c] *M.S. 0755, Sandia National Laboratories, P.O. Box 5800, Albuquerque, NM 87185-0710, USA*

Received 10 December 2002; accepted 20 February 2003

Abstract

The 25% niobium substituted crystalline titanosilicate with the composition $Na_{1.5}Nb_{0.5}Ti_{1.5}O_3SiO_4 \cdot 2H_2O$ (Nb–TS) was synthesized under hydrothermal conditions. Its selectivity for radioactive ^{137}Cs and ^{89}Sr was compared with the TS, $Na_2Ti_2O_3SiO_4 \cdot 2H_2O$, having sitinakite topology. The Nb–TS shows significantly higher uptake value for ^{137}Cs but lower for ^{89}Sr than the TS. To investigate the origin of selectivity, the ion exchanged Cs^+ and Sr^{2+} forms with the composition, $Cs_xNaH_yNb_{0.5}Ti_{1.5}O_3SiO_4 \cdot zH_2O$ ($x = 0.1$, 0.2 and 0.3, $x + y = 0.5$ and $z = 1-2$) and $Sr_{0.2}Na_{0.6}H_{0.5}Nb_{0.5}Ti_{1.5}O_3SiO_4 \cdot H_2O$, respectively, were structurally characterized from the X-ray powder diffraction data using the Rietveld refinement technique. Simultaneously the kinetics of ^{137}Cs and ^{89}Sr uptake was investigated for the Nb^V free and doped samples. While the Cs^+ and Sr^{2+} exchanged form of Nb–TS and the Cs^+ exchanged form of TS retain the symmetry of the parent compound, the Sr^{2+} exchanged form of TS undergoes a symmetry change. The differences in the uptake of Cs^+ and Sr^{2+} result from the different coordination environments of cesium and strontium in the eight-ring channel, that result from various hydration sites in the tunnel. The origin of selectivity appears to arise from the higher coordination number of cesium or strontium. Other effects due to Nb^V substitution are reflected in the increase of both, the *a*- and *c*-dimensions and thus the unit cell volume, and the population of water vs. Na^+ in the channel to charge-balance the $Nb^{5+} \leftrightarrow Ti^{4+}$ substitution.

Keywords: Titanosilicate; Niobium; Structure; Rietveld analysis; Ion exchange; Selectivity; Distribution constant; Uptake; Cesium; Strontium

1. Introduction

The efforts to build the atomic bomb and sustain a nuclear weapons race during the cold war resulted in a steep environmental price. Consequential quantities of radioactive contaminants were not only stored at several sites but also released into the environment [1–3]. One of the effective strategies to minimize the nuclear waste volumes for final disposal is the selective separation of ^{90}Sr and ^{137}Cs [4]. However, the low concentration of these radioactive elements in a solution that has high sodium ion content (up to 6 M) and alkalinity, renders this a daunting task.

Inorganic ion-exchangers are useful for selective removal and safe storage of radionuclides from mixed nuclear waste due to their high radiation stability and extreme selectivity [5–8]. The industrially produced form of crystalline titanosilicate (referred to as TS henceforth) with the mineral sitinakite topology (referred to as CST for crystalline silicotitanate in the literature), UOP IONSIV® IE-911 (UOP, Inc. Des Plains, IL.) has been under investigation at various DOE waste-managing sites such as Westinghouse Savannah River Technology Center as a baseline technology for removal of radioactive ^{137}Cs from tank wastes [9]. In the work carried out at Sandia National Laboratories, [10–12] it was found that the selectivity of TS for Cs^+ is greatly enhanced by partial substitution of Nb^{5+} for Ti^{4+} (up to 25%) in the framework. However the chemical and/or structural origin of this selectivity has never been investigated. Recently, Luca et al reported Nb^V substitution in the sitinakite framework and its influence on Cs^+ ion exchange [13]. They postulated multiple cesium

*Corresponding author. Fax: +1-979-845-2370.
E-mail address: Clearfield@mail.chem.tamu.edu (A. Clearfield).

0022-4596/03/$ - see front matter © 2003 Elsevier Science (USA). All rights reserved.
doi:10.1016/S0022-4596(03)00145-2

environments in the samples with and without framework Nb^{V} based on the results of ^{133}Cs NMR. Emphasizing the need for further experiments to clearly define water structure in the channels of Cs^{+} exchanged sitinakite, they stated, "These different Cs^{+} environments are clearly dependent on the amount of water in the channels [13]."

Previous structural studies on different tunnel type titanium silicates, have shown that isotypic substitution of Ti^{IV} by Ge^{IV} in the framework octahedral and/or tetrahedral (T) sites can result in framework charge modifications, unit cell changes, phase changes and changes in the location of extra-framework cations [14,15]. These changes can in turn modify the ion-exchange capacity and stability of the material thus giving a handle to tune them. In the case of aluminosilicate zeolites silicon substitution by germanium results in aluminogermanate frameworks with Ge/Al ratios close to one and several novel sites for extra framework cations. In the process the ion exchange capacity is enhanced over the isotypic zeolites with $Si/Al > 1$ [16].

The present structural characterization was carried out in order to pinpoint the different hydration water coordination environments of Cs^{+} and Sr^{2+} ions that influence the selectivity upon Nb^{V} substitution in TS besides other changes that are outlined above. The reader should keep in mind the limitation, that an average structure determined through X-ray diffraction in the presence of static disorder of the tunnel constituents and their statistical occupancy of multiply closed sites, lacks a precise and complete determination of all the atoms and water molecules. The preliminary studies on the distribution constants and uptake by the 25% Nb^{V}-substituted sample with the composition $Na_{1.3}H_{0.2}Nb_{0.5}Ti_{1.5}O_3SiO_4 \cdot 2H_2O$ (referred as Nb–TS henceforth) confirmed the reported observations of significantly higher uptake for Cs^{+} by Anthony et al. [10,11]. However, the sample showed lower values of uptake for Sr^{2+} when compared with the TS. Since the structure of Sr^{2+} exchanged forms has not been reported for these materials, we undertook a systematic investigation to determine the origin of such a difference in selectivity in this tunnel type ion-exchanger.

We report here, synthesis, comparative ion exchange behavior of the TS with the 25% Nb^{V}-doped TS and the changes in structure of various Cs^{+} and Sr^{2+} exchanged forms. The distribution constants (K_d), which indicate the selectivity of the ion exchanger towards the particular species was determined in various simulants for Nb–TS and compared with those for TS. Kinetics of recovery of ^{89}Sr and ^{137}Cs from highly alkaline solution containing 5.6 M Na^{+} was also investigated. Uptake of Sr^{2+} and Cs^{+} from neutral solutions in the presence of various amounts of Na^{+} was measured for both types of TS.

2. Experimental

2.1. Synthesis of crystalline titanosilicate (TS) and 25% Nb-substituted crystalline titanosilicate (Nb–TS)

The synthesis of TS was carried out by modifying the hydrothermal reaction that was described previously by Poojary et al. [17]. A total of 6.66 mL of $TiCl_4$ was mixed with 23 ml of doubly distilled (ddi) H_2O and 40 mL of 30% hydrogen peroxide and stirred vigorously. To the stirring mixture, 40 mL of 10 M NaOH was added, followed by 150 mL of ddi H_2O and a solution of 6 mmol of SiO_2 in 1 M NaOH, in that order. Finally, to the resulting clear solution 0.12 mole of NaOH was added. The mixture was sealed in a Teflon lined pressure vessel and kept at 200°C for 10 days. After cooling to room temperature, the solid product was separated by filtration, washed with 1 M NaOH and ethanol, and dried for 24 h at 60°C at air. X-ray powder diffraction of the product revealed the crystalline form of TS.

In the case of Nb–TS, titanium isopropoxide (TIPT, 3.43 g, 12 mmol), tetraethylorthosilicate (TEOS, 3.33 g, 16 mmol) and Nb_2O_5 (0.54 g, 4 mmol Nb) were added to 50 mL aqueous NaOH (6.6 g, 165 mmol) solution in a 100 mL Teflon lined autoclave Parr reactor. To this mixture was added a small amount of previously synthesized seeds of Nb–TS (~0.3 g) to enhance crystallinity and purity of the product and to decrease its crystallization time. The mixture was stirred for 0.5 h, and then placed in a 200°C oven for 3 days. The resulting product, a white microcrystalline powder, was collected by filtration (yield ~2.2 g of $HNa_2Ti_3NbSi_2O_{14} \cdot 4H_2O$; 86% yield based on Ti^{IV}). A small amount of crystalline byproduct was inevitably formed with the major Nb–TS product. Before analyses of the sample, the byproduct was removed by a two step treatment: first, the Nb–TS with the byproduct was exposed to a 1 M aqueous HCl wash for three hours at room temperature, and secondly, the resulting solid was then exposed to a 1 M NaOH wash for three hours at 40°C. The first step amorphizes the byproduct, and the second step dissolves the resulting amorphous material.

2.2. Ion exchange: preparation of Cs^{+} and Sr^{2+} exchanged samples

A series of Cs-exchanged Nb–TS materials were prepared by ion exchange. The maximum amount of Na in Nb–TS that can be readily exchanged for Cs was approximately 25%. For each ion exchange, 3 g of Nb–TS was combined with 50 mL aqueous CsCl solution, containing the appropriate amount of CsCl to obtain a Cs-exchange Nb–TS sample with 3.8, 6.4, 9.0 and 9.6 wt% cesium. The Nb–TS samples were shaken with

the CsCl solutions at room temperature for 12 h, and the Cs-exchanged samples were collected by filtration. Inductively coupled plasma mass spectroscopy (ICP MS) was used for compositional analysis of these Cs-exchanged Nb–TS materials. Powder X-ray diffraction was used for phase identification, purity and crystallinity, and thermogravimetric analysis (TGA) was used to determine water content.

Strontium exchange in Nb–TS was performed in a similar fashion as the Cs^+ exchange. A total of 400 mg of dried sample was equilibrated with 100 mL of 0.025 M solution of $SrCl_2$ for 12 h. The solid was separated by filtration, rinsed with ethanol and dried in the oven for 12 h at 60°C. An exact amount of dry sample was dissolved in HF and the solution was analyzed for Sr and using atomic-absorption (AA) spectroscopy. The calculated composition, $Sr_{0.19}Na_{0.61}HNb_{0.5}Ti_{1.5}O_3SiO_4 \cdot H_2O$, determined using AA spectroscopy, TGA and charge neutrality, closely matched the composition obtained by X-ray diffraction analysis.

2.3. Distribution coefficients and uptake measurements: materials and methods

All chemicals were purchased from commercial sources and used as such without further purification. All ion-exchange experiments were performed by the batch method. About 40 mg of dry ion exchanger was equilibrated with 10 mL of the solution of interest at ambient temperature in 25 mL polyethylene vials for 24–48 h. Samples were filtered out through Acrodisk LC 13 mm syringe filter with 0.2 μm polyvinylidene fluoride (PVDF) membrane. Filtrates were analyzed for either Sr or Cs by various techniques depending on the type of the experiment.

2.4. Absorption measurements of Sr^{2+} and Cs^+ in the presence of $NaNO_3$

In the present study we determined uptake of Sr^{2+} and Cs^+ from the solutions having different Na^+ concentrations. In order to simulate the concentrations of the actual nuclear wastes, we prepared solutions using non-radioactive metals with concentrations high enough that would make ion-exchangers saturated to their maximum capacity by the target ion. In particular, we prepared 5 solutions with 340–350 ppm of Sr^{2+} and 5 solutions with 630–770 ppm of Cs^+. The sodium ion concentrations were 0, 0.5, 1.0, 2.5 and 5.0 M. The exchange was carried out for 24 h as described above. Amounts of Sr^{2+} and Cs^+ in solutions were analyzed by AA spectroscopy and the pHs of the solutions were measured using an Ion Analyzer 250 with glass electrode. Uptake of the cations was calculated as follows:

$$U = \frac{(C_o - C_{eq}) \times 10}{m \times M \times 10^3}, \quad (1)$$

where U is the uptake of the cation, meq/g, M the mass of the gram-equivalent of the cation, g/eq, C_o, C_{eq} the concentrations of starting and final solutions, ppm, m the mass of the ion-exchanger, g.

2.5. Kinetic studies

Kinetics of the removal of ^{89}Sr and ^{137}Cs from radioactive waste type solutions was examined using the radioactive tracer method. Solutions were prepared by dissolving appropriate amounts of $NaNO_3$ and NaOH in ddi H_2O to give 4.27 M $NaNO_3$ and 1.33 M NaOH and then spiked by either the ^{137}Cs or the ^{89}Sr isotope. Solids were batch-equilibrated with the solutions as described above during various periods of time. Activity of ^{137}Cs and ^{89}Sr in the filtrates were measured using a Wallac 1450 liquid scintillation counter (LSC). Recovery, R, of the nuclide at each point of time was calculated as follows:

$$R = \frac{A_0 - A_{eq}}{A_0} \times 100\%, \quad (2)$$

where A_0 is the activity of the starting solution, cpm/mL, A_{eq} the activity of solution at equilibrium, cpm/mL.

2.6. Assessment of ion exchange properties of the materials in nuclear waste type solutions

In order to assess the behavior of the ion-exchangers in nuclear wastes solutions, distribution constants (K_d) for ^{137}Cs and ^{89}Sr were determined in alkaline simulants with various Na^+ contents. Two sets (6 solutions each) were prepared for Sr and Cs series. Each of the solutions in the Cs and Sr set was spiked by ^{137}Cs and ^{89}Sr, respectively. The volume activity of the solutions was about 500–600 cps/mL. All solutions were 1 M in NaOH and 0–4.5 M in $NaNO_3$. The equilibrating time was 24 h. Filtrates were analyzed by counting on LSC. K_d values in mL/g were calculated as follows:

$$K_d = \frac{A_0 - A_{eq}}{A_{eq}} \times \frac{10}{m}. \quad (3)$$

2.7. X-ray powder diffraction data collection, structure solution, and Rietveld refinement

X-ray powder data were collected for six samples: $H_{0.5}NaNb_{0.5}Ti_{1.5}O_3SiO_4 \cdot 2H_2O$ (Nb–TS), $Cs_{0.1}H_{0.4}NaNb_{0.5}Ti_{1.5}O_3SiO_4 \cdot 2H_2O$ (Cs1–Nb–TS), $Cs_{0.2}H_{0.3}NaNb_{0.5}Ti_{1.5}O_3SiO_4 \cdot H_2O$ (Cs2–Nb–TS), $Cs_{0.3}H_{0.2}NaNb_{0.5}Ti_{1.5}O_3SiO_4 \cdot 2H_2O$ (Cs3–Nb–TS), $Sr_{0.2}Na_{0.6}H_{0.5}Nb_{0.5}Ti_{1.5}O_3SiO_4 \cdot H_2O$ (Sr–Nb–TS) and $Sr_{0.33}HNa_{0.34}Ti_2O_3SiO_4 \cdot 2H_2O$ (Sr–TS).

The samples were packed into a flat plastic sample holder and data were acquired in Bragg–Brentano geometry by means of a Bruker-D8 advance computer-automated X-ray diffractometer. The X-ray source was a sealed tube operating at 40 kV and 40 mA with a copper target. Data were collected at room temperature between 8.5° and 85° in 2θ with a step size of 0.02° and a count time of 60 s/step. The powder patterns of the Nb–TS and its Cs^+ and Sr^{2+} exchanged samples were similar to TS. They were indexed using the program NTREOR incorporated in the program EXPO [18,19]. The solution, which indexed all the peaks, corresponded to a tetragonal cell with cell parameters close to, $a \sim 7.83$ Å and $c \sim 11.94$ Å in all the cases. The systematic absences were consistent with the space group $P4_2/mcm$, previously reported for TS [17]. The powder pattern of Sr–TS showed two distinct peaks at *d*-spacings of 11.758 and 11.041 Å that were not observed in any of the Nb^V substituted or pure TS. Initial studies and preliminary indexing results indicate that this is a mixture of two phases. A detailed structural study of these new phases will be published elsewhere [20].

In the first instance, each data set was treated individually, using the same general procedure described below. The data were analyzed using the Rietveld technique in conjunction with the Generalized Structure Analysis System (GSAS) suite of Larson and Von Dreele [21,22]. Atomic positions reported for the framework atoms of TS were used to model and refine the framework cations of all Nb–TSs [17]. The individual site occupancies for the disordered framework Nb^V and Ti^{IV} atoms were put equal to the ratio determined from the ICP MS (1/3) and their sum was constrained to a value equal to 1. The positions of the Cs^+, Na^+, Sr^{2+} ions and water molecules in each of the structure were obtained by difference Fourier maps, followed by Rietveld refinement of the full patterns. The atomic positions of the framework atoms were refined with soft constraints consisting of both Ti/Nb–O = 2.00(2) Å and Si–O = 1.63(2) Å as bonded distances in the Nb^V/Ti^{IV} octahedra and Si tetrahedra respectively and O–O = 2.66(2) Å as non-bonded distances in the silicate tetrahedra [23]. No bond distance constraints were applied for the refinement of alkali and alkaline earth metal ions and water oxygen positions. During the final cycles of refinement, the weight of the soft constraints was reduced, and was finally lifted without reducing the stability of the refinement. In all the cases the isotropic thermal parameters of the framework species were set equal to one another, as were those of the non-framework cations, with both sets allowed to vary independently in the later stages of the refinement. The background was subtracted by means of a shifted Chebyshev polynomial background function consisting of 10 to 12 terms. Histogram scale factor, lattice constants and zero point shifts were also introduced to pinpoint reflection positions. The diffraction peaks were modeled using a Pseudo-Voigt function with Gaussian, Lorentzian, line broadening and asymmetry correction terms. Neutral-atom scattering factors were used for all atoms. No corrections were made for anomalous dispersion, absorption, or preferred orientation.

A series of refinements was set up in which the position and occupancy of the Na^+, Cs^+, Sr^{2+} and water were examined for all the five cases. The process indicated that Na1 fully occupied the framework site $(0, \frac{1}{2}, \frac{1}{2})$ in all the Cs^+ exchanged samples. However, in the case of Sr–Nb–TS, this site is only 71.3(2)% occupied. In the case of Cs2–Nb–TS and Cs3–Nb–TS, two partially occupied sites in the eight-ring tunnel were observed for Cs^+ ions at $(\frac{1}{2}, \frac{1}{2}, x)$ with $x = \frac{1}{4}$ and ~ 0.126, as reported by Poojary et al. [17]. However only one site in the tunnel at $(\frac{1}{2}, \frac{1}{2}, \frac{1}{4})$, partially occupied by Cs^+ ions was observed for low cesium substituted, Cs1–Nb–TS. The water molecules were found at different locations and their environment and occupancy will be discussed for each of the samples below.

During the final cycle of refinement all positional and thermal parameters, profile coefficients, background, unit cell, and diffractometer zero parameters were varied. The weight of the soft constraints was reduced gradually to zero and a stable refinement persisted. The occupancy of Cs^+ and water molecules were fixed close to the values calculated on the basis of ICP MS and TG analysis, respectively. The refinement results show that the cations and the lattice water molecules in these phases exhibit relatively larger thermal parameters, possibly due to disorder or partial occupancy.

The results of the individual X-ray data sets with the final positional and thermal parameters for the five samples are given in Tables 1–5. Selected bond lengths for all samples except Nb–TS are given in Table 6 whereas bond angles for Cs3–Nb–TS and Sr–Nb–TS are given in Table 7. Bond lengths for Nb–TS and bond angles for Nb–, Cs1–Nb, Cs2–Nb–TS have been submitted as supplementary information. The final observed and calculated diffraction profiles of the Rietveld refinement of only Nb–TS and Cs3–Nb–TS are displayed in Figs. 1 and 2 and they represent changes in the diffraction pattern upon cesium substitution. Results of the Rietveld refinement of Cs1–, Cs2– and Sr–Nb–TS have been submitted as supplementary information.

3. Results

3.1. Ion exchange properties: absorption measurements under neutral conditions Cs^+ uptake measurements

The experimental values of the uptake of Cs^+ ions by pure and Nb–TS as a function of sodium ion

Table 1
Refined fractional atomic coordinates and isotropic displacement parameters (Å^2) for Nb–TS

Atom	Site	x	y	z	B	Occ.[a]
Ti/Nb	8*o*	0.1392(2)	0.1392(2)	0.1541(2)	1.812	0.75/0.25
Si	4*e*	0	0.5	0.25	1.812	1
O1	16*p*	0.1195(9)	0.3876(8)	0.1710(5)	1.812	1
O2	8*o*	0.1126(8)	0.1126(8)	0.3295(8)	1.812	1
O4	4*i*	0.1445(12)	0.1445(12)	0	1.812	1
Na1	4*f*	0	0.5	0.5	1.812	1
OW1	4*j*	0.2744(13)	0.2744(13)	0.5	3.765	1
OW2	8*o*	0.4479(15)	0.4479(15)	0.1117(13)	3.765	0.5

$a = 7.8331(4)$ Å, $c = 12.0074(7)$ Å.
$\chi^2 = 6.368$.
$R_{F2} = 9.01\%$, w$R_p = 9.09\%$, $R_p = 7.95\%$.
[a] Occupancy.

Table 2
Refined fractional atomic coordinates and isotropic displacement parameters (Å^2) for Cs1–Nb–TS

Atom	Site	x	y	z	B	Occ.
Ti/Nb	8*o*	0.1407(2)	0.1407(2)	0.1547(2)	1.500	0.75/0.25
Si	4*e*	0	0.5	0.25	1.500	1
O1	16*p*	0.1316(7)	0.3873(6)	0.1721(4)	1.500	1
O2	8*o*	0.1121(8)	0.1121(9)	0.3324(9)	1.500	1
O4	4*i*	0.1486(9)	0.1486(9)	0	1.500	1
Na1	4*f*	0	0.5	0.5	1.500	1
Cs1	2*d*	0.5	0.5	0.25	6.316	0.08
OW1	4*j*	0.2894(12)	0.2894(12)	0.5	6.316	1
OW2	8*o*	0.4443(9)	0.4443(9)	0.1105(9)	6.316	0.5

$a = 7.8339(4)$ Å, $c = 12.0339(5)$ Å.

Table 3
Refined fractional atomic coordinates and isotropic displacement parameters (Å^2) for Cs2–Nb–TS

Atom	Site	x	y	z	B	Occ.
Ti/Nb	8*o*	0.1418(2)	0.1418(2)	0.1528(2)	1.163	0.75/0.25
Si	4*e*	0	0.5	0.25	1.163	1
O1	16*p*	0.1382(8)	0.3935(7)	0.1675(5)	1.163	1
O2	8*o*	0.1154(6)	0.1154(6)	0.3344(7)	1.163	1
O4	4*i*	0.1564(11)	0.1564(11)	0	1.163	1
Na1	4*f*	0	0.5	0.5	1.163	1
Cs1	2*d*	0.5	0.5	0.25	5.465	0.3
Cs2	4*h*	0.5	0.5	0.1263(15)	5.465	0.1
OW1	4*j*	0.2824(12)	0.2824(12)	0.5	5.465	0.5
OW2	4*j*	0.5916(25)	0.5916(25)	0.5	5.465	0.5

$a = 7.8397(4)$ Å, $c = 12.0321(6)$Å.

Table 4
Refined fractional atomic coordinates and isotropic displacement parameters (Å^2) for Cs3–Nb–TS

Atom	Site	x	y	z	B	Occ.
Ti/Nb	8*o*	0.1400(1)	0.1400(1)	0.1531(1)	1.810	0.75/0.25
Si	4*e*	0	0.5	0.25	1.810	1
O1	16*p*	0.1222(4)	0.3870(4)	0.1662(3)	1.810	1
O2	8*o*	0.1153(4)	0.1153(4)	0.3266(4)	1.810	1
O4	4*i*	0.1494(6)	0.1494(6)	0	1.810	1
Na1	4*f*	0	0.5	0.5	1.810	1
Cs1	2*d*	0.5	0.5	0.25	6.521	0.42
Cs2	4*h*	0.5	0.5	0.1582(9)	6.521	0.12
OW1	4*j*	0.2451(2)	0.2451(2)	0.5	6.521	0.5
OW2	4*i*	0.4264(1)	0.4264(1)	0	6.521	0.5
OW3	8*n*	0.2496(17)	0.3473(12)	0.5	6.521	0.5

$a = 7.8690(2)$ Å, $c = 12.0890(3)$Å.
$\chi^2 = 1.626$.
$R_{F2} = 4.17\%$, w$R_p = 8.54\%$, $R_p = 6.65\%$.

Table 5
Refined fractional atomic coordinates and isotropic displacement parameters (Å^2) for Sr–Nb–TS

Atom	Site	x	y	z	B	Occ.
Ti/Nb	8*o*	0.1435(3)	0.1435(3)	0.1548(3)	1.326	0.75/0.25
Si	4*e*	0	0.5	0.25	1.326	1
O1	16*p*	0.1256(13)	0.3978(14)	0.1663(7)	1.326	1
O2	8*o*	0.1190(8)	0.1190(8)	0.3234(9)	1.326	1
O4	4*i*	0.1559(11)	0.1559(11)	0	1.326	1
Na1	4*f*	0	0.5	0.5	1.326	0.737
Sr1	4*j*	0.3969(19)	0.3969(19)	0	3.302	0.197
OW1	4*j*	0.2683(20)	0.2683(20)	0.5	3.302	1

$a = 7.8463(2)$ Å, $c = 11.9985(6)$ Å.

concentration are plotted in Fig. 3. For Na^+ concentrations ranging from 0 to 5 M, Nb–TS shows higher uptake values in agreement with those observed by Dosch and Anthony [10,11]. Particularly, in the region of sodium ion concentrations higher than 0.5 M, pure TS picks up almost no Cs^+, whereas Nb–TS shows much higher uptake especially in solutions with high ionic strength. Equilibrium pH values of Cs^+ solutions are plotted in Fig. 4. Though both the curves have similar shape, the pH for Nb–TS solution is lower. This may be attributed to partial hydrolysis. Metal ion forms of TS type materials could be considered as insoluble salts formed by a strong base such as those of alkali metals and a very weak insoluble acid $H_2Ti_2O_3SiO_4 \cdot 2H_2O$. The hydrolysis of the sodium form of TS type material in water solutions could be described by the following reaction:

$$\overline{Na}^+ + HOH \Leftrightarrow \overline{H}^+ + Na^+ + OH^-. \quad (4)$$

According to Le Chatlier's principle the equilibrium can be altered by changing the concentration of sodium and hydroxonium ions in the solution as well as the amount of sodium ions, residing within the framework of the ion exchanger. The increase of Na^+ concentration causes the downward slope of both curves because equilibrium shifts to the left. The amount of hydrolyzable sodium ions is also crucial for equilibrium. Since the amount of sodium ions in Nb–TS is 15% less than in pure TS, under similar conditions, the pH of the Nb–TS equilibrium solution is lower.

Table 6
Selected interatomic distances (Å)

Cs1–Nb–TS		Cs2–Nb–TS		Cs3–Nb–TS		Sr–Nb–TS	
Nb/Ti (Oh) Polyhedra							
Oh–O1	1.951(5) × 2	Oh–O1	1.981(5) × 2	Oh–O1	1.954(3) × 2	Oh–O1	2.004(12) × 2
Oh–O2	2.167(8)	Oh–O2	2.204(8)	Oh–O2	2.115(5)	Oh–O2	2.041(11)
Oh–O2	2.006(4) × 2	Oh–O2	2.033(5) × 2	Oh–O2	2.033(3) × 2	Oh–O2	2.085(12) × 2
Oh–O4	1.868(2)	Oh–O4	1.846(3)	Oh–O4	1.854(2)	Oh–O4	1.863(2)
Si Polyhedra							
Si–O1	1.655(5) × 4	Si–O1	1.690(5) × 4	Si–O1	1.655(3) × 4	Si–O1	1.619(8) × 4
Non-framework cations							
Na1–O1	2.483(5) × 4	Na1–O1	2.436(6) × 4	Na1–O1	2.399(4) × 4	Na1–O1	2.366(10) × 4
Na1–O4	3.000(4) × 2	Na1–O4	2.960(4) × 2	Na1–O4	2.999(2) × 2	Na1–O4	2.964(7) × 2
Na1–OW1	2.814(2) × 2	Na1–OW1	2.794(2) × 2	Na1–OW1	2.7827(4) × 2	Na1–OW1	2.781(2) × 2
				Na1–OW2	2.303(12) × 2		
Cs1–O1	3.171(6) × 8	Cs1–O1	3.119(6) × 8			Sr1–O1	2.91(2) × 4
		Cs1–OW2	3.175(9) × 4	Cs1–O1	3.264(3) × 8	Sr1–O4	2.67(3)
		Cs2–O1	2.998(7) × 4	Cs1–OW2	3.132(4) × 4	Sr1–OW1	2.81(2) × 2
		Cs2–OW1	2.95(1) × 2	Cs2–O1	3.104(3) × 4		
				Cs2–OW1	3.421(19) × 4		
				Cs2–OW3	2.998(12) × 2		

Table 7
Selected bond angles (°)

Cs3–Nb–TS		Sr–Nb–TS	
Nb/Ti (Oh) Polyhedra (O–Oh–O)			
O1–Oh–O1	97.82(20)	O1–Oh–O1	97.8(7)
O1–Oh–O2	90.22(16)	O1–Oh–O2	91.1(4)
O1–Oh–O2	164.9(2)	O1–Oh–O2	165.4(5)
O1–Oh–O2	90.81(13)	O1–Oh–O2	90.8(5)
O1–Oh–O4	92.56(19)	O1–Oh–O4	91.2(5)
O2–Oh–O2	77.37(20)	O2–Oh–O2	76.9(5)
O2–Oh–O2	78.29(21)	O2–Oh–O2	78.6(7)
O2–Oh–O4	175.7(3)	O2–Oh–O4	176.5(9)
O2–Oh–O4	99.39(22)	O2–Oh–O4	100.4(6)
Si Polyhedra (O–T–O)			
O1–Si–O1	104.6(2)	O1–Si–O1	103.4(7)
O1–Si–O1	108.9(2)	O1–Si–O1	105.0(8)
O1–Si–O1	115.0(2)	O1–Si–O1	120.6(8)
Nb/Ti (Oh) Polyhedra (Oh–O–Oh)			
Oh–O2–Oh	100.0(2)	Oh–O2–Oh	99.6(7)
Oh–O2–Oh	101.6(2)	Oh–O2–Oh	102.0(5)
Oh–O2–Oh	173.6(4)	Oh–O4–Oh	171.6(13)

3.2. Sr^{2+} uptake measurements

The experimental values of uptake of Sr^{2+} by pure and Nb–TS plotted against sodium ion concentration are shown in Fig. 5. Unlike Cs^{+} uptake, the Sr^{2+} absorption shows two distinct regions. Below 1.0 M Na the uptake of Sr^{2+} in Nb–TS is higher but in more concentrated solutions pure TS behaves better than Nb–TS. In particular, the uptake value of Sr^{2+} from 5 M sodium ion solutions is twice as much for pure TS than for Nb–TS. The pH curves for Sr^{2+} solutions look similar for both the materials (Fig. 6). As in the case of Cs^{+} the equilibrium pH values are generally lower for Nb–TS. The pH remains nearly neutral for solutions with high sodium ion content in the case of Nb–TS. The hydrolysis is suppressed and only ion exchange occurs.

3.3. Kinetic studies

The recovery of ^{89}Sr and ^{137}Cs as a function of time was studied from alkaline media to compare the kinetics of Sr^{2+} and Cs^{+} uptake for Nb–TS and the TS phase. A total of 5.6 M Na^{+} was present as a competitive ion for the framework sites. As observed in Fig. 7, the kinetics of recovery of ^{89}Sr from such a solution is the same both for Nb- and pure TS. In both the systems the equilibrium was reached in 20 min, and no more nuclide was recovered from solution after that. Also, both the materials used up to ~90% of their equilibrium uptake for ^{89}Sr under these conditions in 1 min. However, it can be emphasized that, pure TS removed almost 99.6% of ^{89}Sr from solution compared to 85.3% removal by Nb–TS. The K_d values at equilibrium were 60,000 mL/g for pure TS and about 1500 mL/g for Nb–TS. The recovery curve for pure TS is shifted 15 units up compared to the Nb–TS curve. The similarity in the shape of the curves suggests that although $Nb^{5+} \leftrightarrow Ti^{4+}$ substitution increased the tunnel capacity, it did not affect Sr diffusion rates inside the tunnel.

The ^{137}Cs uptake experiments indicated that Cs^{+} was not absorbed by TS in measurable quantity from solution with high sodium content (5.6 M Na^{+}). In the case of pure TS, differences in the remaining activity of the Cs^{+} solution at each point of time did not exceed the counting error. Almost no Cs^{+} was picked up after

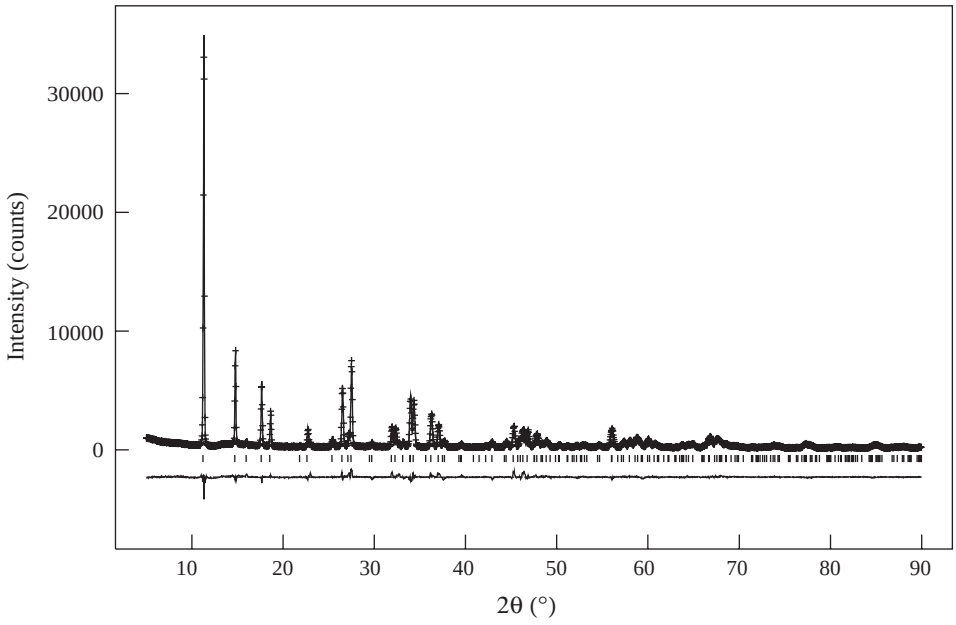

Fig. 1. Results of the Rietveld refinement of the structure of Nb–TS using powder X-ray diffraction data at 298 K. Calculated (full line), experimental (+), and difference (bottom) profiles as well as Bragg reflection positions (tic marks) are shown on the same scale.

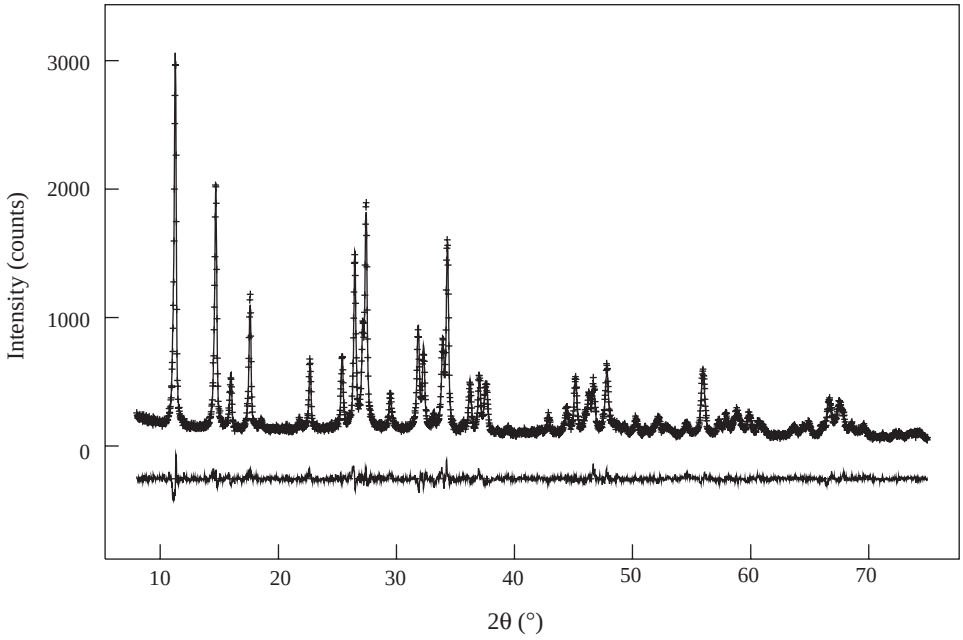

Fig. 2. Profiles derived from the refinement of X-ray diffraction data collected at 298 K for Cs3− Nb–TS.

2 hours of equilibration. Unlike ^{89}Sr uptake, the Nb–TS phase exchanged to only 40% of its final (120 min point in Fig. 7) amount of ^{137}Cs after 1 min, and then in 2 h, 80% of all ^{137}Cs was recovered from the solution. The recovery value continued to increase after 60 min (Fig. 7) implying that the kinetics of ion exchange of Cs^+ in Nb–TS is much slower than that for Sr^{2+}. As Cs^+ is larger than Sr^{2+}, its diffusion rate is expected to be lower than that of Sr^{2+} as shown by the data [23].

In order to assess the behavior of the ion-exchangers in nuclear waste solutions distribution constants (K_d) for ^{137}Cs and ^{89}Sr were determined in alkaline simulants with varying Na^+ concentration. In all the solutions the concentration of NaOH was 1 M. In addition, $NaNO_3$ was added to each solution, so that the concentration in the simulants varied from 0 to 4.5 M. The Cs and Sr simulants for K_d value determination were spiked by ^{137}Cs and ^{89}Sr respectively so that the initial activity of

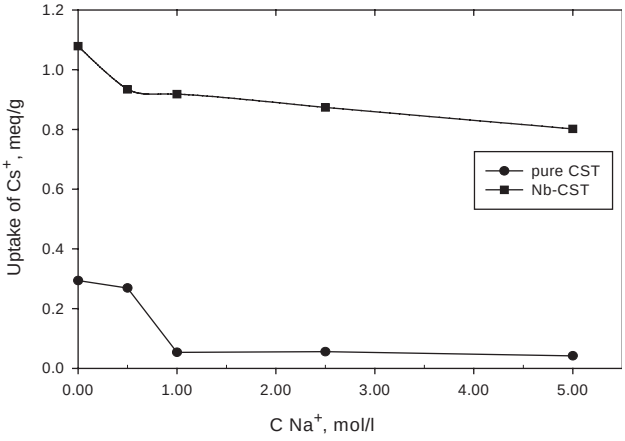

Fig. 3. Uptake of Cs^{+} in sodium form of pure and Nb–TS from neutral solutions.

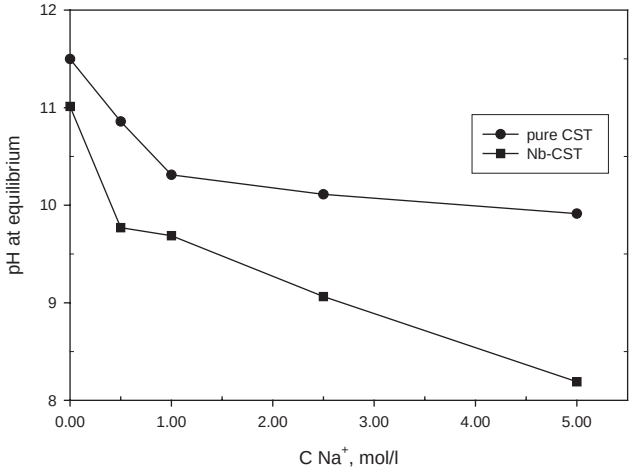

Fig. 4. pH of Cs^{+} solutions at equilibrium.

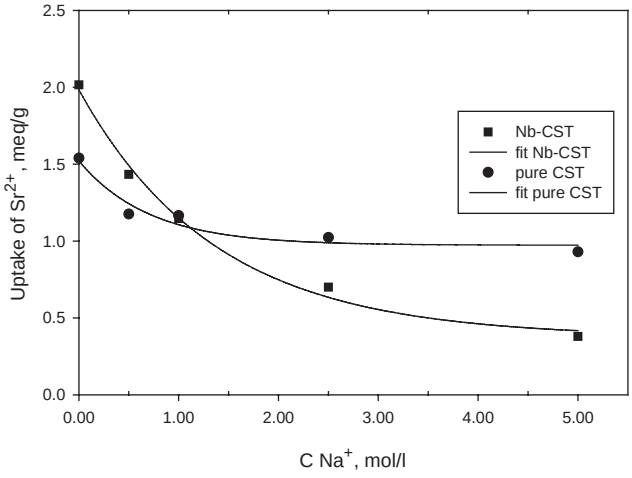

Fig. 5. Uptake of Sr^{2+} in sodium form of pure and Nb–TS from neutral solutions.

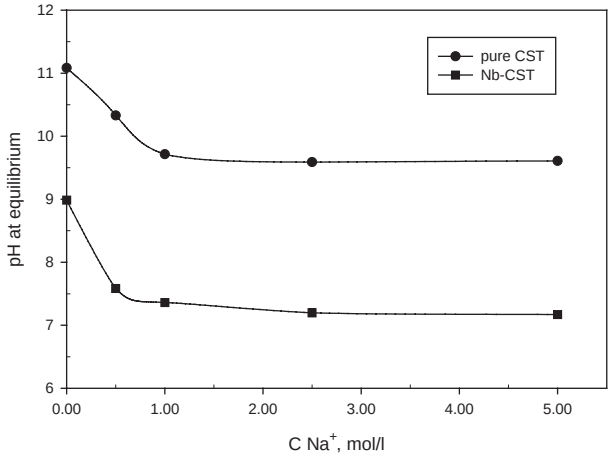

Fig. 6. pH of Sr^{2+} solutions at equilibrium.

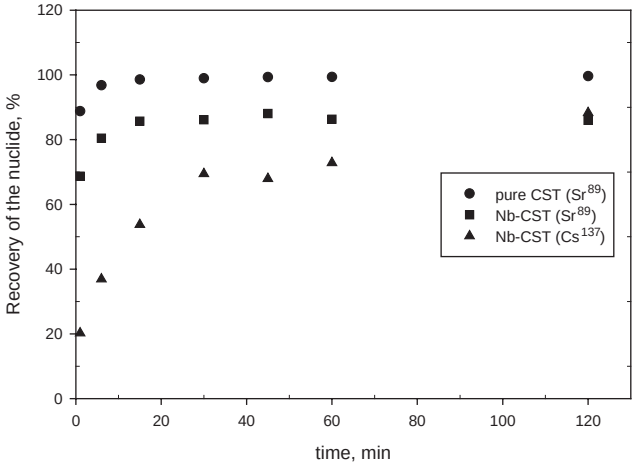

Fig. 7. Kinetics of uptake of radioactive nuclides from solution with high sodium content (5.6 M Na^{+}) in TS and Nb–TS.

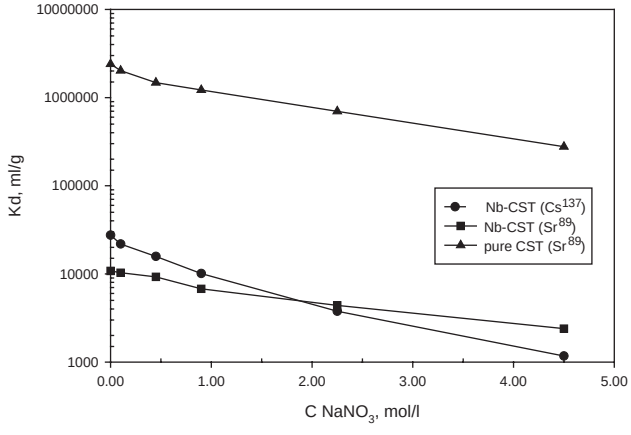

Fig. 8. Kd values for Nb–TS and pure TS from 1 M NaOH solution as a function of $NaNO_3$ concentration. Plot for pure TS (Cs^{137}) is not shown due to very low values of K_d.

the solutions is ca. 2000 times higher than the background.

Fig. 8 shows the plots of experimental K_d values of Nb–TS and pure TS for Cs and Sr against $NaNO_3$ concentration in the simulant. All simulants were 1 M in NaOH to begin with, so the total Na^{+} concentration is $(n+1)$ M, where n-molarity of $NaNO_3$. As evident from

the curves, the Nb–TS is more selective for Cs^+, compared with the pure TS. The K_d value of Cs^+ for Nb–TS in 1 M NaOH is about 23000 mL/g, which is 24 times higher than that for pure TS. This ratio holds up to a concentration of 2 M $NaNO_3$, however, at higher concentrations both materials lose their ability for Cs^+ uptake. The distribution constants show a reversed situation in the case of Sr^{2+}. Pure TS outperforms Nb–TS with a K_d value of 25×10^6 mL/g at 1 M NaOH, and 5×10^5 mL/g at 4.5 M $NaNO_3$/1 M NaOH compared with 12,000 and 200 mL/g in similar conditions for Nb–TS.

3.4. Structure of Nb–TS and ion exchanged forms: origin of selectivity

The tunnel structure of TS with the ideal formula, $Na_2Ti_2O_3SiO_4 \cdot 2H_2O$ and having the mineral sitinakite topology has been described in detail previously [17,24]. Briefly, the structure consists of Ti octahedra occurring in clusters of four and sharing edges to form a cubane like unit. The clusters are connected to each other along *a* and *b* axis by silicate tetrahedra whose oxygen atoms form part of the cluster (Fig. 9). The crystals are tetragonal with $a \approx 7.8$ Å and $c \approx 12.0$ Å. Along the *c*-axis the titania-clusters are connected through oxo-bridging (Fig. 11). This arrangement forms a framework enclosing a one-dimensional tunnel parallel to the *c*-axis direction. There are two crystallographic positions for the eight Na^+ ions in the unit cell. Half of the sodium ions reside within the framework at $(0, \frac{1}{2}, \frac{1}{2})$ bonded to four silicate oxygen atoms and two water molecules. The remaining sodium ions reside in the tunnels at (x, x, z) with $x \sim 0.435$, $z \sim 0.059$) with partial occupancies as these positions are close to themselves. Instead, protons substitute for Na^+ ions and the actual formula is $Na_{1.64}H_{0.36}Ti_2O_3SiO_4 \cdot 1.84H_2O$. There are two water sites in TS. For the Cs^+ exchanged sample, $Na_{1.49}Cs_{0.2}H_{0.31}Ti_2O_3SiO_4 \cdot H_2O$, the framework Na^+ are retained, while the tunnel is occupied by two types of disordered Cs^+ ions; Cs1 at $(\frac{1}{2}, \frac{1}{2}, \frac{1}{4})$ and Cs2 at $(\frac{1}{2}, \frac{1}{2}, z)$ with $z \sim 0.131$. The Cs1 forms an eight-coordinated complex with framework oxygens (O1) while Cs2 forms a six-coordinated complex with four framework oxygens (O1) and two water molecules (OW1). There is only one water site in this case. Though, the overall framework structure of Nb–TS (Fig. 9) and its Cs^+ and Sr^{2+} exchanged forms is similar to TS with the same space group, the non-framework cations and water distribution is different. The unit cell dimensions are larger than TS due to the 25% Nb^V in the framework. They also become progressively larger in the Nb^V substituted series with increasing Cs^+ substitution and different hydration levels. In all the samples framework Nb^V cations were disordered with Ti^{IV} in an octahedral environment and Na^+ are located in the ac faces of the framework at $(\frac{1}{2}, 0, \frac{1}{2})$ and $(0, \frac{1}{2}, \frac{1}{2})$ etc.

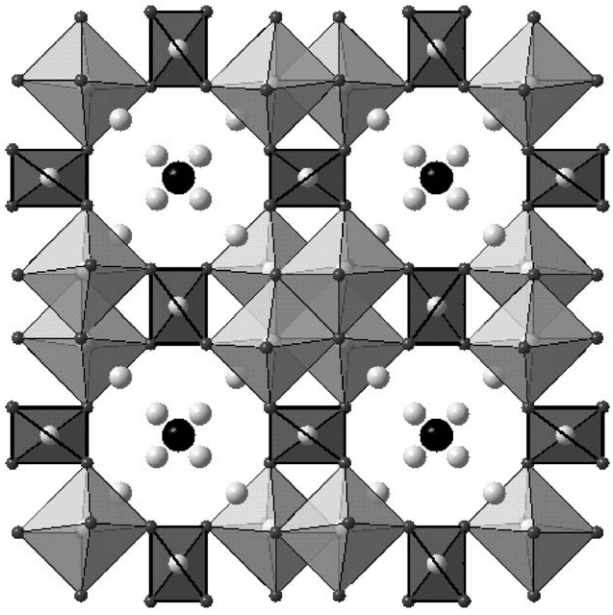

Fig. 9. A polyhedral representation of the crystal structure of Cs exchanged Nb–TS with the sitinakite topology along [001]. The dark and light grey spheres represent Cs^+ cations and water molecules, respectively.

In the case of Nb–TS, two types of water molecules and protons occupy the channel sites (Table 1). The site at $(x, x, \frac{1}{2})$ with $x \sim 0.275$ is fully occupied by water molecules, OW1. These water molecules are involved in bonding to the framework sodium. The other water sites at (x, x, z) with $x \sim 0.45$ and $z \sim 0.11$ is partially occupied by water molecules OW2. In the absence of Cs^+ an electron density was also observed at $(\frac{1}{2}, \frac{1}{2}, \frac{1}{4})$ in the difference Fourier. This can be attributed to water or minor amounts of Na^+. The refinement became unstable on including either of these species. The Na^+ ions are expected to have low refined occupancy of only 0.07 because the 25% Nb^V substitution for Ti^{IV} reduces the tunnel Na^+ content exclusively. Protons can also replace Na^+ by hydrolysis as noted previously by Poojary et al. [17]. The volume expansion of 1% above that of the TS phase is due to the combined effect of Nb^V substitution and the presence of 8% more water molecules. Thus, the more realistic formula incorporating the presence of protons, ICP, MS, TG analysis and based on X-ray refinement would be $H_{0.5}NaNb_{0.5}Ti_{1.5}O_3SiO_4 \cdot 2H_2O$. A total weight loss of 11.1% based on TGA experiments matches closely with a calculated weight loss of 11.32%.

In the case of Cs1–Nb–TS, the channel sites are partially occupied by a Cs^+ ion and two types of water molecules (Table 2). Only one site containing the water molecules was observed in the case of TS. The water positions are similar to those observed for the Na–TS sample described above. The water site, OW1, is fully

occupied and this water bonds with Na1. The occupancy of site with disordered OW2 was refined close to 60%. In conjunction with TGA and the closeness of the site to itself and Cs1, the occupancy was fixed at the 50% level. OW2 is hydrogen bonded to residual protons and framework oxygen atoms. The Cs1 forms an eight-coordinated complex with framework oxygens similar to the one observed in the case of TS (Table 6). A direct comparison of volume change cannot be made in this case as TS with a similar composition has not been reported. The TGA results were consistent with the amount of water in the formula, $Cs_{0.1}H_{0.4}NaNb_{0.5}Ti_{1.5}O_3SiO_4 \cdot 2H_2O$, based on the refinement.

Cs2–Nb–TS ($Cs_{0.2}NaH_{0.3}Nb_{0.5}Ti_{1.5}O_3SiO_4 \cdot H_2O$) has a similar composition as the Cs–TS, $Cs_{0.2}Na_{1.49}H_{0.31}Ti_2O_3SiO_4 \cdot H_2O$ (Table 3). The 5.86 $Å^3$ (0.79%) increase of volume over TS can be attributed solely to 25% Nb substitution as the hydration level remains same. Two partially occupied water sites were located in the difference Fourier. The water OW1 at $(x, x, \frac{1}{2})$ with $x \sim 0.273$ is bonded to Cs2 and Na1 with similar environment as observed in the case of OW1 in TS. However, OW2 at $(x, x, \frac{1}{2})$ with $x \sim 0.591$ has no reported equivalent in the case of TS. The statistically occupied Cs1 ion has a different coordination environment in the tunnel than the eight-coordinated Cs1 in the case of TS. Assignment of an exact coordination number (CN) for Cs1 is not possible due to the disordered OW2. The CN number varies from eight to twelve based upon the bonding with eight O1 atoms of the framework at a distance of 3.119(6) Å and four disordered waters at 3.175(9) Å (Table 6). The six-coordinate complex around Cs2 consisting of four framework oxygens and two water molecules (OW2) is similar to the Cs2 in TS. The two water sites are statistically occupied as they are close to each other.

The maximum Cs^+ exchanged sample Cs3–Nb–TS with the composition, $Cs_{0.3}H_{0.2}NaNb_{0.5}Ti_{1.5}O_3SiO_4 \cdot 2H_2O$, shows further difference in the water sites and consequently the cesium environment in the tunnel (Table 4). The volume increase is 9.12 $Å^3$ (1.22%) over the Cs2–Nb–TS and can be attributed to both, the increase in water content in the tunnel, and the Cs occupancy. Three statistically occupied water sites were observed, among them two are novel and have not been previously reported. The water, OW1, at $(x, x, \frac{1}{2})$ with $x \sim 0.24$ is similar to OW1 as observed in the case of Cs–TS. The second water, OW2 at $(x, x, 0)$ with $x \sim 0.426$ is in a four-fold site and is involved in bonding with Cs1 whereas OW3 at an eight fold site $(x, y, \frac{1}{2})$ is bonded to Na1, Cs1 and Cs2. The six-coordinate oxygen environment around Na1 remains the same as in the TS, though in this case it is bonded to two statistically occupied water molecules instead of one fully occupied water molecule in TS. The two statistically occupied Cs^+ ions have completely different hydration water environments compared with Cs^+ ions in TS and in the low Cs substituted Nb–TS discussed above. Cs1 is bonded to eight O1 atoms at 3.264(3) Å and four OW2 at 3.132(4) Å (Table 6). Unlike the Na1 case where the two sites containing the disordered water are mutually exclusive, these two sites containing water with 50% water population can be simultaneously occupied. Although, it is difficult to assign an exact CN to Cs1 due to the statistical nature of the waters, OW2 and OW3, a CN of 12 can be assigned to Cs1 as shown in Fig. 10, based on bond valence calculations [25]. The other disordered Cs2 ion is also located along the tunnel but is displaced 1.109(10) Å away along the *c*-axis from Cs1 compared with 1.425 Å in the case of TS. It is difficult to assign an exact coordination number to Cs2 also. It has a bonding environment with four oxygens of the framework, two OW1 and four OW3. The waters, OW1 and OW3 are too close to be simultaneously occupied. In this case a CN of eight can be assigned based on bond valence calculations [25].

In the Sr^{2+} exchanged sample of Nb–TS, a seven-coordinate Sr was observed at $(x, x, 0)$ with $x \sim 0.3977$ (Table 5, Fig. 11). This site is close to the O4 oxygen connecting two Nb^V/Ti^{IV} octahedra in the six rings formed along [100] by four Nb^V/Ti^{IV} octahedra and two Si tetrahedra (Tables 5 and 6). Unlike other Cs–Nb–TS samples the framework Na site is only partially (73%) occupied in this case. There is only one water site containing OW1. The Sr^{2+} exchange resulted in a mixture of phases in the case of TS [20]. Preliminary

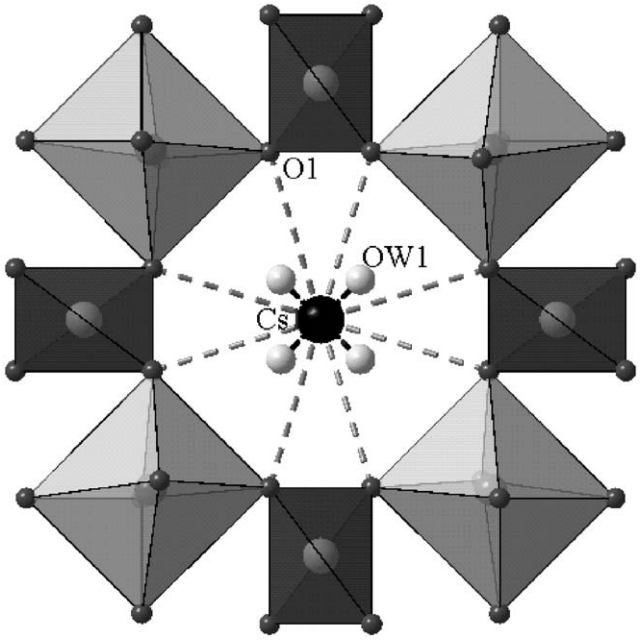

Fig. 10. A polyhedral representation of the eight-ring tunnel of Nb–TS depicting the 12-coordinate environment around Cs1 along [001]. The Cs1 in TS forms an eight-coordinate complex with framework oxygens only.

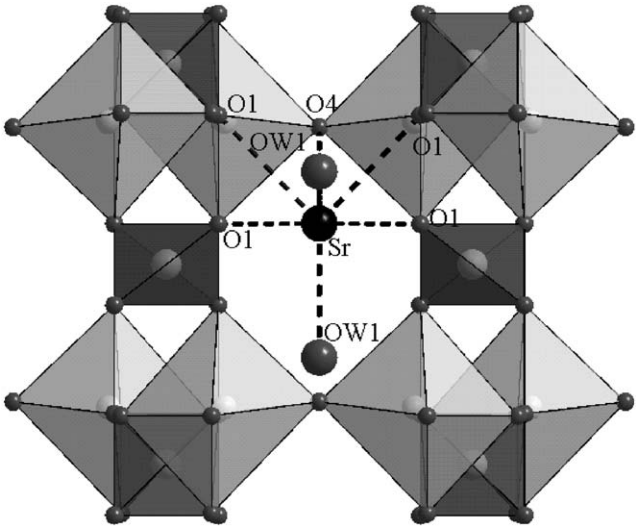

Fig. 11. A polyhedral representation of the six-ring of Nb–TS depicting the seven-coordinate environment around Sr along [100]. The Sr in TS forms a ten-coordinate complex.

results from structure solution of the two phases indicate a mixture of tetragonal and orthorhombic phases. The tetragonal phase has a ten-coordinate Sr [20].

4. Discussion

The eight ring tunnel in the pure and Cs^+-exchanged Nb–TSs, has different water hydration levels and environments. Consequently various cesium coordinations are observed in the three Cs^+ exchanged samples for both the $2d$ ($\frac{1}{2}$, $\frac{1}{2}$, $\frac{1}{4}$) and the $4h$ ($\frac{1}{2}$, $\frac{1}{2}$, z) positions. Several novel hydration water sites in the Nb–TSs reported in this study depend on the purity of the sample, ion exchange conditions, exposure of sample to moisture and amount of Cs substitution. Recently Luca et al. [13] reported the existence of different Cs^+ environment in Nb–TS and high Cs^+ exchanged TS based on an NMR study. The samples reported in this study show minor compositional differences as the impurity reported by them in the Nb–TS sample was isolated and pure samples were prepared. We compared Nb–TSs with the Cs–TSs reported by Poojary et al. [17] and no attempts were made to prepare higher Cs substituted TS. Indeed this average structural analysis using X-ray powder diffraction method is insufficient to pinpoint all the water sites due to static disorder of the tunnel constituents (particularly Na^+ cations and water molecules) and their statistical occupancy of multiply closed sites. However, the study shows that a key factor in the selectivity for a metal ion is the coordination environment around it. The 25% Nb^V substitution for Ti^{IV} results in 25% less Na^+ in the tunnel (Eq. (5)), thus facilitating the uptake of extra water, possibly as a hydrated Cs complex, into the less crowded tunnels.

$$Na^+ + Ti^{4+} \leftrightarrow Nb^{5+}. \quad (5)$$

As the Cs^+ uptake increases, the protons/hydronium ions are displaced from the tunnel which in turn modifies the amount and coordination by water molecules. Several additional bonds formed with water in the case of Cs1 and Cs2 result in thermodynamically more favorable complexes in the case of Nb–TS compared with the TS. The results are consistent with the higher uptake of Cs^+ in Nb–TS compared with TS.

The situation is reversed in the case of Sr^{2+} exchange samples. It appears that the ten-coordinated Sr complex in TS [20] results in the observed higher exchange capacity over the Nb–TS which has a seven-coordinated Sr complex. Unlike Cs^+ ion which occupied the central position in the eight-ring tunnel, the Sr^{2+} cation in Nb–TS is located in the smaller six rings. This site is less spacious for a large amount of water molecules to reside in. In-situ ion-exchange studies are being conducted at the National Synchrotron Light Source in Brookhaven National Laboratory to detail the mechanism of Sr^{2+} exchange in the TS. The two phases that are formed upon Sr^{2+} exchange in TS can be isolated separately if the mechanism of this exchange is known.

5. Conclusion

The increase in Cs^+ selectivity in crystalline TS with the sitinakite topology upon the substitution of Nb^V into the framework Ti^{IV} site was noted and exploited; but the chemical or structural origin of this selectivity has never been investigated. Further, the Sr^{2+} exchange resulted in a complete reversal of selectivity. Structural studies via Rietveld refinement were carried out to detail the origin of such selectivity. Although both the crystallographically unique Cs^+ ions fit in the center of the eight-ring tunnel in Nb–TS and TS, we believe it is the increase in their coordination from eight to twelve for Cs1 and six to ten for Cs2 in Nb–TS that is responsible for the observed behavior. This increase in Cs^+ coordination is possible due the replacement of Na^+ by H_2O in the channel sites to charge-compensate the Ti^{4+}/Nb^{5+} substitution. The water hydration level appears to be dependent upon the amount of Cs^+ in the tunnels. The decrease of Na^+ in the tunnels should also decrease the charge repulsion and is therefore responsible for the increase in Cs^+ exchange capacity of the Nb–TS over TS. However, the depopulation of Na in the channels does not seem to affect the kinetics of Cs sorption, in that the rate was the same for TS and Nb–TS.

In the case of Sr^{2+} exchange, a phase change upon Sr^{2+} absorption results in the formation of a compound

with a ten-coordinate strontium complex in TS as opposed to a seven-coordinate strontium complex in the isostructural 25% Nb–TS. Structural details of Sr^{2+}-exchanged TS phase and its comparison with the Sr^{2+} exchanged Nb–TS will be forthcoming in a separate publication [20]. Our initial results of Sr^{2+} exchange on the two TSs show again that higher coordination of the exchanged-in cation in the tunnel is correlated with higher selectivity for that cation.

Acknowledgments

We gratefully acknowledge the US Department of Energy, Environmental Management Science Program Grant No. DE-FG07-01ER6300 with funds supplied through Westinghouse Savannah River Technology Center.

References

[1] A. Dyer, Mineral. Soc. Ser. 9 (2000) 319.
[2] D.L. Illman, Chem. Eng. News 9 (1993).
[3] E.K. Wilson, Chem. Eng. News 300 (1997) 30.
[4] T.A. Todd, K.N. Brewer, J.D. Law, D.J. Wood, T.G. Garn, R.D. Tillotson, P.A. Tullock, E.L. Wade, WM'97 Proceedings, Vol. 2–6, Tucson, Arizona, 1997, p. 2368.
[5] A. Clearfield (Ed.), Inorganic Ion Exchange Materials, CRC Press, Boca Raton, FL, 1982.
[6] P. Sylvester, E.A. Behrens, G.M. Graziano, A. Clearfield, Sep. Sci. Technol. 34 (1999) 1981.
[7] A.I. Bortun, L.N. Bortun, D.M. Poojary, O. Xiang, A. Clearfield, Chem. Mater. 12 (2000) 294.
[8] T. Moller, R. Harjula, Sep. Sci. Technol. 36 (2001) 885.
[9] W.R. Wilmarth, D.D. Walker, F.F. Fondeur, S.D. Fink, M. Nyman, J. Krumhansl, J.T. Mills, V.H. Dukes, B.H. Croy, WSRC-TR 00221, 2001.
[10] R.G. Anthony, R.G. Dosch, C.V. Philip, WO9419277.
[11] R.G. Anthony, R.G. Dosch, C.V. Philip, US Patent 6, 110, 378, Method of Using Novel Silico-titanates, Sandia National Laboratories, 2000.
[12] R.G. Anthony, C.V. Philip, R.G. Dosch, Waste Manage. 13 (1993) 503.
[13] V. Luca, J.V. Hanna, M.E. Smith, M. James, D.R.G. Mitchell, J.R. Bartlett, Microporous Mesoporous Mater. 55 (2002) 1.
[14] E.A. Behrens, D.M. Poojary, A. Clearfield, Chem. Mater. 10 (1998) 959.
[15] A. Clearfield, Solid State Sci. 3 (2001) 103.
[16] A. Tripathi, J.B. Parise, Microporous Mesoporous Mater. 52 (2002) 65.
[17] D.M. Poojary, R.A. Cahill, A. Clearfield, Chem. Mater. 6 (1994) 2364.
[18] A. Altomare, J. Foadi, C. Giacovazzo, A.G.G. Moliterni, M.C. Burla, G. Polidori, J. Appl. Cryst. 31 (1998) 74.
[19] A. Altomare, C. Giacovazzo, A. Guagliardi, A.G.G. Moliterni, R. Rizzi, P.-E. Werner, J. Appl. Crystallogr. 33 (2000) 1180.
[20] O. Xiang, A. Clearfield, manuscript in preparation.
[21] H.M. Rietveld, Acta Crystallogr. 22 (1967) 151.
[22] A.C. Larson, R.B. Von Dreele, Generalized Structure Analysis System (GSAS), MS-H805, Los Alamos, NM 87545, 1990.
[23] R.D. Shannon, Acta Crystallogr. A 32 (1976) 751.
[24] E.V. Sokolova, R.K. Rastsvetaeva, V.I. Andrianov, Y.K. Egorov-Tismenko, Y.P. Men'shikov, Dok. Akad. Nauk SSSR 307 (1989) 114.
[25] N.E. Brese, M. O'Keeffe, Acta Crystallogr. B 47 (1991) 192.